Thermal-Structural Design/Analysis of an Airframe-Integrated Hydrogen-Cooled Scramjet

Allan R. Wieting* and Robert W. Guy†
NASA Langley Research Center, Hampton, Va.

This paper presents the salient features of a preliminary thermal-structural design and analysis study of a hydrogen-fueled, regeneratively cooled, airframe-integrated scramjet. This three-dimensional fixed geometry scramjet concept, which was developed at NASA Langley Research Center, is designed to operate over a flight Mach number range from 4 to 10. The thermal-structural study was focused on a scramjet application to one concept for a hypersonic research vehicle and was based on technology developed under the NASA Hypersonic Research Engine Project. State-of-the-art analytical methods consisting of lumped system and finite-difference steady-state thermal analyses and a finite-element structural analysis were used. The results of the study indicated that this scramjet concept is viable from both a structural mass and cooling requirement standpoint. However, advances in material and fabrication technology for hydrogen-cooled structures appear necessary for acceptable engine life for commercial application.

Nomenclature

A_c = scramjet module geometric capture area, 0.249 m^2 (2.68 ft^2)
L = overall engine length, 3.63 m (143 in.)
M = Mach number
p = pressure, Pa (psi)
q = dynamic pressure, Pa (psf)
$\dot{q}$ = aerodynamic heating rate, W/m^2 (Btu/ft^2-sec)
T = temperature, K (°R)
ΔT = temperature difference, K (°R)
x,y,z = coordinate axis, m (in.)
X,Y,Z = overall component length in respective coordinate direction, m (in.)
σ = maximum principal stress, Pa (psi)
ϕ_c = coolant equivalence ratio, ratio of the coolant flow rate to the fuel flow rate
ϕ_f = fuel equivalence ratio, ratio of actual flow to fuel flow required for stoichiometric combustion

Subscripts

a = aerodynamic skin
s = primary structure

Introduction

DURING the past decade, research on concepts for hypersonic airbreathing engines has forecast superior performance for hydrogen-burning scramjets (supersonic combustion ramjets) provided that sufficient technology is developed in certain key areas, particularly structures, thermal protection, and airframe integration.[1-5] The NASA Langley Research Center is conducting a research program that is focused on the development of airframe-integrated scramjet concepts (see Fig. 1). These concepts utilize the entire undersurface of the aircraft to process the engine airflow. The aircraft forebody serves as an extension of the engine inlet, and the afterbody serves as an extension of the engine nozzle. A fundamental goal of the program is to evolve an engine with acceptable performance which requires only a fraction of the total fuel heat sink for engine cooling. To attain this goal, the wetted wall areas and heat-transfer rates (especially in the combustor) have been reduced as much as practical consistent with adequate engine performance. Low wetted areas in the combustor require multiple fuel injection planes (struts) to obtain short fuel mixing and combustion lengths.[6] Heat-transfer rate reduction requires large combustor exit-to-entrance area ratios to reduce the pressure in the combustor.[6]

As part of this program, the aerothermodynamic lines for a sweptback, fixed-geometry, hydrogen-fueled, rectangular scramjet module have been defined (see Fig. 1). Analytical performance results[6] indicate that the concept has high potential performance and should have a cooling requirement that is less than the heat sink available in the hydrogen fuel up to at least a flight Mach number of 10. Furthermore, for a Mach 6 cruise flight, the projected cooling requirement is less than half of the available heat sink in the fuel, which results in new vistas for actively cooled airframe structures. However, it should be noted that the cooling predictions are based on estimates of required heat transfer through the engine walls and do not correspond to a realistic, less-than-ideal, fuel/coolant circuit and system design.

Therefore, a preliminary thermal-structural design/analysis study[7] was undertaken to determine, within state-of-the-art technology, the design feasibility of this scramjet concept for a life of 100 hr and 1000 thermal cycles and to determine the associated coolant requirements and structural mass. This study utilized technology similar to that of the NASA Hypersonic Research Engine (HRE) project[8,9] and a hydrogen-cooled panel study[10] and was focused on a potential application to a hypersonic research vehicle.[2] This paper presents the salient features of the thermal-structural design/analysis study.

Engine Description

As a focal point, the scramjets were sized for one concept of a hypersonic research vehicle that has a takeoff gross mass of 29,000 kg (65,000 lb). The aircraft is 23 m (76 ft) long and requires six scramjet engines, which are located 14.8 m (48.6 ft) from the aircraft nose. Two inner scramjet modules are shown in Fig. 1; the sidewall of one module is removed to reveal the internal engine surfaces. The scramjet module for this application is 0.56 m (22 in.) high, 0.447 m (17.6 in.) wide, and has an overall length of 3.63 m (143 in.). A general

Submitted Dec. 20, 1974; presented as Paper 75-137 at the AIAA 13th Aerospace Sciences Meeting, Pasadena, Calif., Jan. 20-22, 1975; revision received April 28, 1975. The authors are grateful to J.A. Butler of NASA Langley Research Center and J.D. Beadling of LTV Aerospace Corporation, who performed the NASTRAN analysis.

Index category: Airbreathing Propulsion, Hypersonic.

*Aero-Space Technologist, Design Concepts Section, Thermal Structures Branch, Structures and Dynamics Division.

†Aero-Space Technologist, Advanced Facilities Research Section, Hypersonic Propulsion Branch, High-Speed Aerodynamics Division.

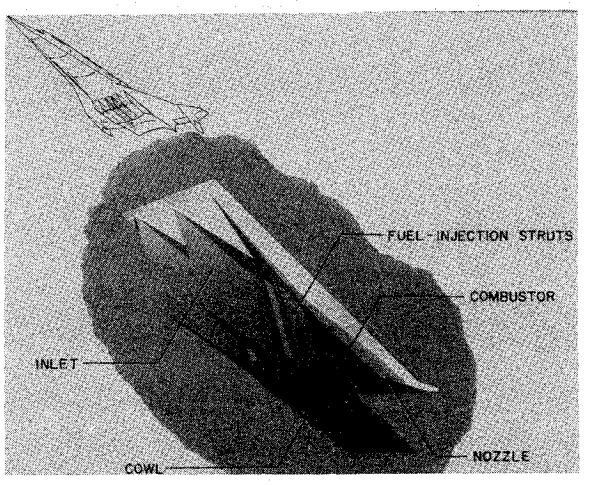

Fig. 1 Airframe-integrated scramjet concept.

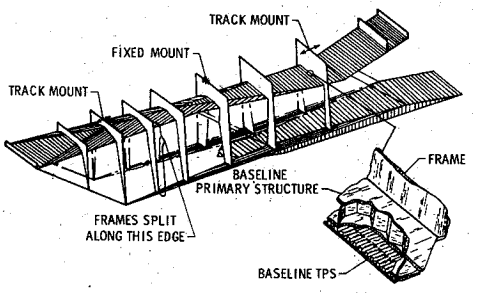

Fig. 2 Baseline engine thermal-structural concept.

description of the engine geometry and the results of aerothermodynamic performance analyses are given in Ref. 6.

Conceptual Design

During the conceptual design phase of this study, baseline thermal-structural concepts, materials, and design criteria were established based on technology developed primarily in the NASA Hypersonic Research Engine (HRE) Project[8,9] and a hydrogen-cooled panel study.[10] To provide accessibility and replaceability of parts, each scramjet module has four major structural components: top, cowl, sidewall (common to adjoining scramjet module), and the three fuel injection struts. The two side struts are identical, asymmetric, and have 3/2 the chord of the symmetric center strut.

Thermal Protection System

All engine surfaces wetted by the engine internal airstream are cooled regeneratively by circulating the hydrogen fuel through a thermal protection system along the surfaces prior to injecting it into the stream. The baseline thermal protection system (TPS) (see Fig. 2) consists of a brazed rectangular offset-fin plate-fin surface heat exchanger made of Hastelloy X (HRE baseline). The offset-fin plate-fin surface heat exchanger offers excellent heat-transfer characteristics[11] in addition to permitting some degree of crossflow (due to offset fins) and thereby preventing coolant starvation in the event of blockage of a coolant passage. Nominal TPS dimensions are as follows: aerodynamic skin thickness, 0.38 mm (0.015 in.); fin height, 1.27 mm (0.050 in.); fin thickness, 0.15 mm (0.006 in.); and fin offset length, 2.5 mm (0.10 in.).

Coolant Routing

In general, the coolant is introduced at the component leading and trailing edges (low heat load areas) and flows longitudinally (basically parallel to airflow) toward the component center (engine throat area and highest heat load area), where it is collected in manifolds and routed to a fuel plenum.

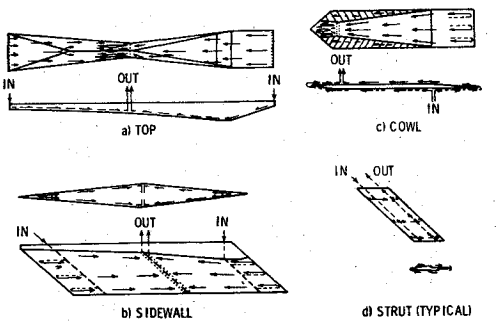

Fig. 3 Scramjet coolant routing scheme.

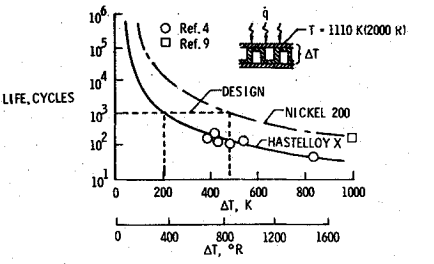

Fig. 4 Thermal cycle life of offset-fin heat exchanger.

From there, it is dispersed to the fuel manifolds in each strut and injected into the airstream. The coolant routing scheme for each component is shown in Fig. 3. This routing scheme minimizes the temperature variation transverse to the flow direction, the temperature differential through the surface heat exchanger, and the aerodynamic heat load, thereby reducing the cooling requirements. Two coolant circuits per component were necessitated by the fuel pressure requirement, as frictional pressure losses for one circuit would be excessive. The outlets of the two circuits were placed together, since calculations in Ref. 10 indicate that the resulting temperature distributions will minimize thermal stresses.

All leading edges exposed to stagnation heating from the airflow are impingement cooled. The coolant is injected through a slot in the coolant inlet manifold and impinges on the inside surface of the leading edge, which then turns the coolant around to flow along the component surface (see Fig. 3 b). The impingment cooling technique augments the coolant heat-transfer characteristics along the stagnation line by a factor of 2 to 3.[12]

A unique feature of this routing scheme is the commonality of the cooling circuits for the sidewall component of adjoining scramjet modules. This minimizes any temperature differential across the sidewall component, thereby reducing thermal stresses and warpage.

Primary Structure

The baseline primary structures are frame-stiffened honeycomb panels for the engine shell (sidewalls, top, and cowl) and solid plates for the fuel injection struts (see Fig. 2). Inconel 718 is the baseline material. The honeycomb panel has 0.38- and 0.76 mm- (0.015- and 0.030 in.-) thick face sheets, a core depth of 6.4 mm (0.25 in.), and the core cross-sectional area is 10% of the face sheet area. The frames are nominally 2.5 mm (0.10 in.) thick and 25 cm (10 in.) apart.

Design Conditions

This scramjet operates over a flight Mach number range from 4 to 10, with ascent at a constant dynamic pressure of 72 kPa (1500 psf) and cruise at a nominal dynamic pressure of 28 kPa (580 psf). The engines are designed for the maximum loading conditions, which occur during 3-g maneuvers at a

dynamic pressure of 72 kPa (1500 psf) with stoichiometric combustion ($\phi_f = 1.0$). The maximum thermal loading [heating rates up to 5.7 MW/m^2 (500 Btu/ft^2-sec) on plane surfaces] occurs at Mach 10. The maximum aerodynamic pressure loading [pressures up to 1.1 MPa (160 psia)] is transient, occurring during the unstarting (transition from supersonic to subsonic flow) of the engine if the combustor thermally choked at a flight Mach number of 5.2 with stoichiometric combustion. Since the transient pressure pulse was not defined fully, the design pressure loading is taken conservatively as the envelope of the peak transient pressures.[7]

As in the HRE design, the thermal protection system is not considered part of the primary load-carrying structure, as it generally will be in a plastic state by virtue of elevated temperature operation with large temperature differences through its structure. However, it must provide the required life, which is an order of magnitude greater than the HRE. The thermal cyclic life of the baseline TPS[4] (Hastelloy X) is given in Fig. 4. To meet the life criteria, the maximum temperature difference had to be limited to 200 K (360°R); however, this limit could not be attained in all cases. In these cases, a Nickel 200 TPS was used, as it exhibits superior life,[9] as shown in Fig. 4. By virtue of its higher thermal conductivity, Nickel 200 also yields lower temperature differences for a given heat flux; however, Hastelloy X was used as the baseline material wherever possible because of its superior creep properties.

A maximum primary structure temperature limit of 890 K (1600°R) was selected (HRE limit), since the strength of the baseline material deteriorates rapidly above this level. This limit and the maximum allowable temperature difference result in a maximum TPS aerodynamic skin temperature limit of 1090 K (1960°R).

The fuel/coolant is parahydrogen stored cryogenically as a liquid at 20 K (37°R) and 240 kPa (35 psia). A maximum fuel pressure of 4.8 MPa (700 psia) is required to obtain the proper fuel flow rate and penetration into the airstream; this, together with assumed pressure drops of 0.34 MPa (50 psia) in the fuel system and 1.7 MPa (250 psi) in the coolant circuits, results in a coolant supply pressure of 7 MPa (1000 psia). The coolant supply temperature is taken as 110 K (200°R), allowing a conservative margin to account for energy absorbed by the hydrogen as it is pressurized as a liquid from the initial tank condition.

Analytical Methods

Thermal Analysis

The thermal analysis consisted of separate aerodynamic and cooling-system thermal analyses.

Aerodynamic thermal analysis

An integral boundary-layer method developed specifically for application to scramjets[13] was used to calculate the aerodynamic heating rates to the various engine surfaces. Boundary-layer transition was assumed to occur at a momentum thickness Reynolds number of 1000 or at the first shock boundary-layer interaction.

Cooling-system thermal analysis

The primary cooling-system thermal analysis utilized the Colburn-Reynolds' analogy[11] in a steady-state lumped system technique in which the heat transferred by radiation is assumed to be negligible and the aerodynamic heat transferred to the structure is balanced by the heat removed by the coolant. A finite-difference thermal analyzer, Martin Interactive Thermal Analyses System (MITAS),[14] was used for leading-edge regions, local hot spots, and for the fuel injection struts. All fluid properties were evaluated at the hydrogen bulk temperature as recommended[11] for offset-fin heat exchangers. The fin friction and heat-transfer factors

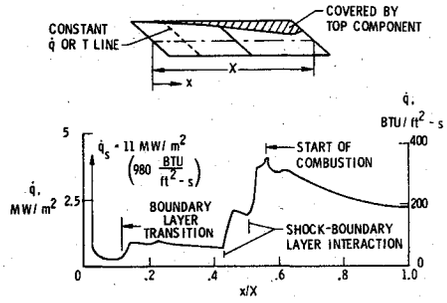

Fig. 5 Aerodynamic heating-rate distribution along sidewall.

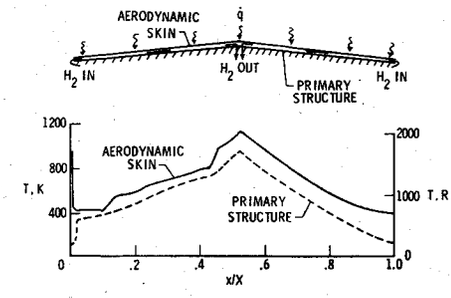

Fig. 6 Temperature distribution along sidewall.

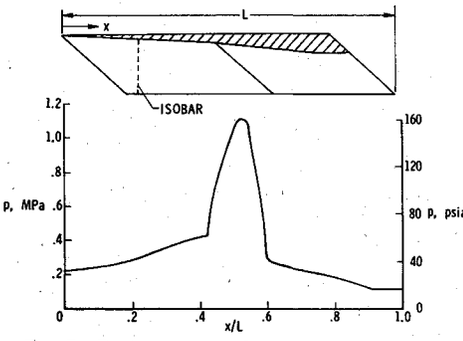

Fig. 7 Design pressure loads for engine sidewall.

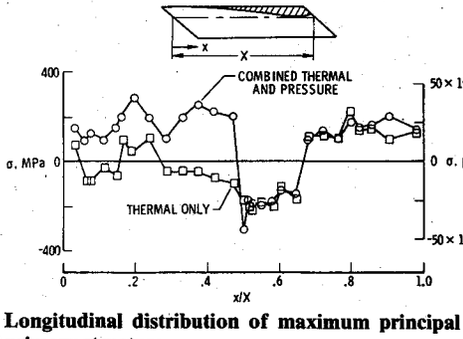

Fig. 8 Longitudinal distribution of maximum principal stresses in sidewall primary structure.

were obtained from empirical relationships developed by correlating experimental data for 22 rectangular offset-fin plate-fin configurations.

Structural Analysis

The finite-element computer program, NASTRAN[15] level 15, was used for the stress analyses under thermal and pressure loadings. The structural temperatures predicted from the thermal analyses were used as input to the thermal stress analysis. The structural analysis of the engine was handled in two parts to reduce the size of the finite-element model. The engine shell, one engine module minus the three fuel injection struts, was one part, and a side strut was the other part. The

side strut only was modeled, as the loading was slightly more cirtical than the center-strut loading, and the results would be conservatively representative for the center strut. Although modeled relatively coarsely, the basic engine shell finite-element model had 3600 unrestrained degrees of freedom, and the side-strut finite-element model had 2600 unrestrained degrees of freedom. These finite-element models were made up primarily of triangular and quadrilateral plate elements with both membrane and bending stiffness.

Results and Discussion

Engine-Airframe Mounting System

Preliminary calculations indicated that excessive thermal stresses would occur if the structure were constrained fully. Therefore, the structure is allowed to expand to relieve the thermal stresses where possible. The overall thermal expansion is accomodated by attaching each scramjet module to the airframe by a three-point system located on the longitudinal centerline of the top surface (see Fig. 2). The center mount is fixed, whereas the mounts near the engine extremities allow the engine module to expand longitudinally. Consequently, each module is free to move longitudinally from the center mount, laterally from the longitudinal centerline, and vertically downward from the top plane. However, the commonality of the sidewall component between adjoining scramjet modules results in lateral expansions being restricted.

To accommodate the lateral expansion, the sidewall frames are split (see Fig. 2). In addition, module cowls are independent and allowed to slip relative to one another. The design features expansion joints and seals at the top and bottom of the sidewall and a sliding seal between the cowls. The leading- and trailing-edge sections of the sidewall remain integral between adjoining scramjet modules; however, by virtue of being in a low-temperature region, the thermal stresses are acceptable. This overall freedom to expand will relieve the thermal stress due to the absolute temperature change from ambient; however, the internal thermal stresses due to the nonlinear temperature profiles are relieved only by minimizing the thermal gradients.

Engine Shell

The sidewall component exemplifies the thermal-structural problems of the baseline engine shell structure. The aerodynamic heating varies considerably due to boundary-layer transition, shock-boundary-layer interactions, and combustion, as shown in Fig. 5. This variation, coupled with the basic nonlinearity of a two-circuit cooling system, since the coolant temperature increases from inlet to outlet, results in the nonlinear aerodynamic surface skin temperature and primary structure (honeycomb panel) temperature distributions shown in Fig. 6.

The primary structure temperature distribution of Fig. 6, in combination with the unstart pressure distribution of Fig. 7, gives the design loading for the sidewall primary structure. Typical results of the stress analysis are shown in Fig. 8. The results indicate that the thermal stresses are the major design factor except in the inlet, where the sidewall is cantilevered and the pressure loading is of equal concern.

Fuel Injection Struts

The fuel injection struts (see Figs. 1 and 9) presented the most formidable cooling and structural problems. They simultaneously had to support a large side load, contain high-pressure hydrogen at two temperature extremes, and withstand the high thermal stresses resulting from asymmetric and nonlinear aerodynamic heating, as well as convective heating from the hot hydrogen in the internal manifolds.

The struts, which have a maximum thickness of 3.35 cm (1.32 in.) and chords of 25 and 38 cm (10 and 15 in.), span 56 cm (22 in.) and are swept back 48°. Each strut is subdivided internally into four longitudinal compartments (see Fig. 9): the fore and aft compartments serve as coolant inlet and outlet manifolds and the central compartments as fuel manifolds for the strut trailing edge (parallel) and wall (perpendicular) fuel injectors. Coolant in the forward manifold is injected through a slot, impinges on the leading edge, and splits (unequally) to flow along each wall to the trailing edge, where it is collected in the aft manifold. The parallel injection mode is not used above $M=7$; consequently, the parallel fuel injection manifold was assumed void of fuel for the thermal analysis.

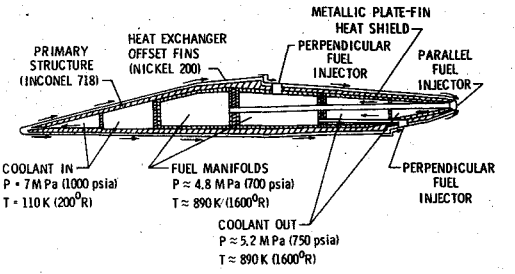

Fig. 9 Typical side-strut cross section (chordwise).

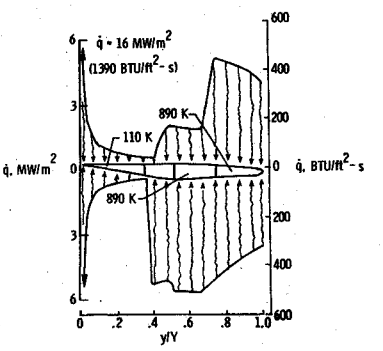

Fig. 10 Aerodynamic heating-rate distribution along each wall of the side strut.

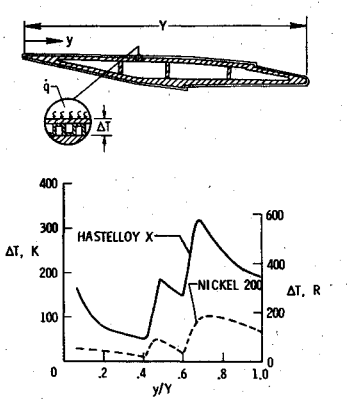

Fig. 11 Temperature difference distribution through baseline Hastelloy X and Nickel 200 thermal protection systems.

Thermal loading

Overall thermal expansions are accommodated by the strut-mounting system. At the top, a three-point suspension is used in which the leading edge is fixed and the other two points have two degrees of freedom each. This system allows the strut to move chordwise from the leading edge and laterally from one side. At the cowl, the strut fits into a slot that allows longitudinal expansion but provides support for side loads.

As shown in Fig. 10, the aerodynamic heating varies considerably along the strut wall as well as from one side to the

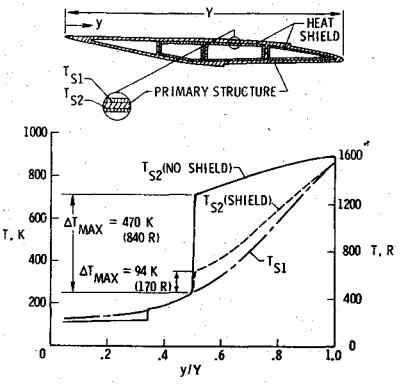

Fig. 12 Primary structure temperature distribution along side-strut side passage wall with and without the internal heat shield.

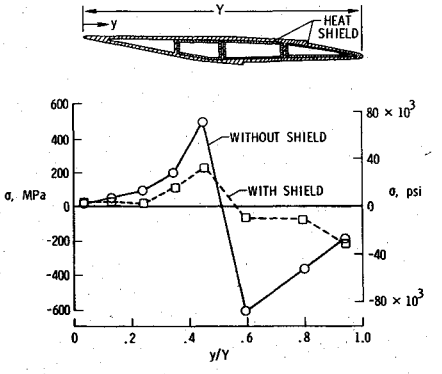

Fig. 13 Typical chordwise maximum principal thermal stress distribution with and without internal heat shield.

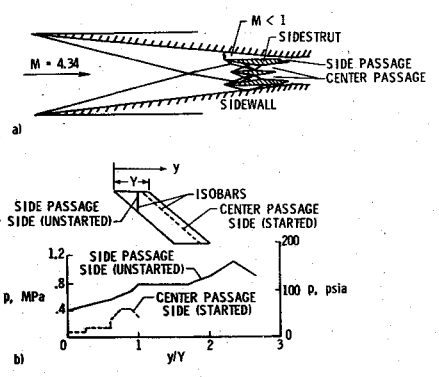

Fig. 14 Schematic of unsymmetrical unstart and external design pressure loading for side strut: a) schematic of unsymmetrical unstart in side passage; b) design pressure loading on side-strut wall during unsymmetrical unstart.

other. Temperature differences as high as 320 K (570°R) [well in excess of the design allowable of 200 K (360°R)] occurred in the baseline Hastelloy X TPS, as shown in Fig. 11. The use of a Nickel 200 TPS reduced the maximum temperature difference to 110 K (200°R), which corresponds to a life well in excess of the design life (see Fig. 4) However, for sustained high-temperature operation, creep becomes important, and the Nickel 200 will not have adequate life. Consequently, advances in material and fabrication technology for hydrogen-cooled structures appear necessary for acceptable engine life for long-term application.

Extreme temperature differences up to 470 K (840°R) through the primary structure wall and thermal stresses up to 80% of the allowable stress were encountered in the structural wall of the strut, as shown in Fig. 12 and 13, respectively. These large temperature differences and stresses were primarily the consequence of internal convective heating from

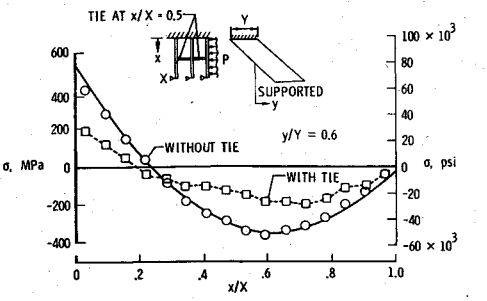

Fig. 15 Typical longitudinal distribution of maximum principal stresses in side-strut wall with and without strut tie.

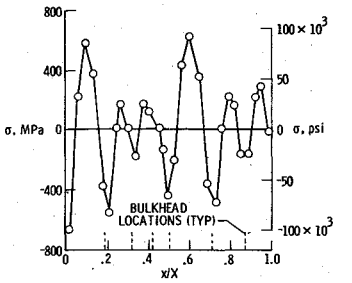

Fig. 16 Typical lateral distribution of maximum principal stresses in side-strut wall due to internal pressure loading.

the hot hydrogen in the manifolds. Attempts to reduce these stresses by rearranging the fuel and cooling manifolds as well as the coolant circuitry proved fruitless. By incorporating a metallic plate-fin heat shield in the hot manifolds, the primary structure temperature differences and thermal stresses were reduced successfully by approximately 64%, as indicated in Fig. 12 and 13, respectively. The heat shield was similar to the plate-fin heat exchanger on the aerodynamic surfaces, but the fins were oriented so as to restrict flow and provide essentially stagnant hydrogen in the passages between the shield and the strut wall, thereby eliminating direct convection heating to the strut wall.

External pressure loading

The maximum external pressure loading occurs when the aerodynamic flow in the passage between the sidewall and side strut unstarts (subsonic flow) and the flow in the other three passages remains started (supersonic flow), as depicted in Fig. 14a. The pressures on each side of the strut are shown in Fig. 14b. This is a conservative loading, as discussed in Ref. 7. On the side-passage wall isobars are vertical with a maximum of 1.1 MPa (160 psia), whereas on the center-passage wall isobars are parallel to the strut leading edge, swept 48° relative to vertical, with a maximum of 0.41 MPa (60 psia) occurring near the trailing edge. The net loading is approximately 0.7 MPa (100 psi) on the side-passage wall of the side strut.

Table 1 Scramjet module component mass and coolant requirement breakdowns

Component	Mass/A_c, kg/m^2(lbm/ft^2)	ϕ_c[a]
Top	204 (41.7)	0.109
Sidewall	480 (98.2)	0.390
Cowl	182 (37.2)	0.234
Struts		
center	29 (6.0)	0.055
side (2)	94 (19.3)	0.188
Total	989 (202.4)	0.976

[a] Based on stochiometric fuel requirements for a 3g maneuver at $M=10$, $q=72$ kPa (1500 psf), and coolant inlet and outlet temperatures of 110 K (200°R) and 890 K (1600°R).

The resulting stresses are as would be expected for a beam fixed at one end with the other end simply supported. The maximum principal stress of approximately 580 MPa (85 ksi) occurs at the fixed end. Combination of these stresses with the thermal stresses results in principal stresses in excess of the design allowable. Inasmuch as the thermal stresses were felt to be a minimum within the design constraints, the three struts were tied together at their midpoint, thereby decreasing the bending stresses due to the external side load. A typical longitudinal distribution of the maximum principal stresses for the side strut with and without a tie is shown in Fig. 15. The tie reduces the maximum stress approximately 50% to acceptable levels.

Internal pressure loading

The internal pressure in each strut compartment is carried primarily in bending by the wall between the compartment bulkheads. The resulting stresses for the design pressure [7 MPa (1000 psia)] are shown in Fig. 16, and, as expected, they indicate almost pure bending in the sidewall elements between bulkheads. The stress levels are excessive; consequently, additional bulkheads will have to be added to reduce the stress levels. Since the loading is indicative of a fixed end beam under uniform load, the addition of one bulkhead per compartment should reduce the stresses by about a factor of 4 to acceptable levels.

Structural Mass and Coolant Requirements

The mass and coolant requirement breakdowns for individual components of a single scramjet module are listed in Table 1. As might be expected, the sidewall component is the heaviest and requires the highest coolant flow rate. From these results, it can be shown that the major scramjet module sections, namely, the inlet, combustor, and nozzle, require 29%, 55%, and 14%, respectively, of the available fuel heat sink capacity at the maximum heat load condition. It should be noted that the coolant maximum heat load predictions do not include coolant requirements for the afterbody of the aircraft which is utilized as a nozzle extension. Typically, this region has large areas subjected to low heat loads and has the potential to reject the heat load by radiation. However, any energy absorbed by the nozzle section should properly be charged to the scramjet coolant requirements.

Although this study is very preliminary in nature, and many significant structural problems remain unsolved, the thermal-structural design of this scramjet concept is felt to be feasible. This scramjet concept is a viable one in that it has a structural mass per unit capture area of 989 kg/m^2 (202.4 lbm/ft^2) and a cooling equivalence ratio (ϕ_c) of 0.98 at the maximum thermal loading condition [$M=10$, $q=72$ kPa (1500 psf), $3g$ maneuver, $\phi_f=1$]. As a comparison, the HRE had a mass per unit capture area of 1500 kg/m^2 (310 lbm/ft^2) and a cooling equivalence ratio of 2.9.

Concluding Remarks

Results of a preliminary thermal-structural design and analysis study of a NASA concept for an airframe-integrated hydrogen-cooled scramjet module indicate that it is possible to attain a life of 100 hr and 1000 thermal cycles, which is the design goal for the intended research application. However, for increased life, advances in fabrication and material technology appear necessary. Furthermore, the scramjet module appears viable from both an engine structural mass and coolant requirement standpoint in that it has a mass per unit capture area of 989 kg/m^2 (202.4 lbm/ft^2) and a coolant equivalence ratio of 0.98 at the maximum thermal loading condition, which occurs at Mach 10 with stoichiometric combustion.

References

[1] Becker, J.V. and Kirkham, F.S., "Hypersonic Transport," Paper 25, NASA SP-292, Nov. 1971.

[2] Henry, J.R. and Beach, H.L., "Hypersonic Air-Breathing Propulsion Systems," Paper 8, NASA SP-292, Nov. 1971.

[3] Bushnell, D.M., "Hypersonic Airplane Aerodynamic Technology," Paper 5, NASA SP-292, Nov. 1971.

[4] Anderson, M.S. and Kelly, H.N., "Structures Technology for Hypersonic Vehicles," Paper 9, NASA SP-292, Nov. 1971.

[5] Edwards, C.L.W., Small, W.J., Weidner, J.P., and Johnston, P.J., "Studies of Scramjet/Airframe Integration Techniques for Hypersonic Aircraft," AIAA Paper 75-58, Pasadena, Calif. Jan. 1975.

[6] Henry, J.R. and Anderson, G.Y., "Design Considerations for the Airframe-Integrated Scramjet," NASA TM X-2895, Dec. 1973.

[7] Wieting, A.R. and Guy, R.W., "Preliminary Thermal-Structural Design and Analysis of an Airframe-Integrated Hydrogen-Cooled Scramjet," AIAA Paper 75-137, Pasadena, Calif. 1975.

[8] Staff of Langley Research Center and AiResearch Manufacturing Company, The Garrett Corporation, "Hypersonic Research Engine Project Status 1971," NASA TM X-2572, 1972.

[9] Staff of AiResearch Manufacturing Company, The Garrett Corporation, "Hypersonic Research Engine Project: Phase II—Structures and Cooling Development, Fourth Interim Technical Data Report," Data Item 55-7.04, AiResearch Rept. AP-68-3250, March 1, 1968 NASA CR-66986.

[10] Walters, F.M. and Buchmann, O.A., "Heat Transfer and Fluid Flow Analysis of Hydrogen-Cooled Panels and Manifold Systems," NASA CR-66925.

[11] Kays, W.M. and London, A.L., *Compact Heat Exchangers*, 2nd ed., McGraw-Hill, New York, 1964.

[12] Livingood, J. N.B. and Gauntner, J.W., "Heat-Transfer Characteristics of a Single Circular Air Jet Impinging on a Concave Hemispherical Shell," NASA TM X-2859, Aug. 1973.

[13] Pinckney, S.Z., "Turbulent Heat Transfer Prediction Method for Application to Scramjet Engines, NASA TN-D-7810, Nov. 1974.

[14] Staff of Martin-Marietta Corporation, "Martin Interactive Thermal Analyses System," Version 1.0, MDS-SPLPD-71-FD238 (REV3), March 1972, Martin-Marietta Corporation. Denver, Colo.

[15] Butler, T.G. and Michel, D., "NASTRAN, A Summary of the Functions and Capabilities of the NASA Structural Analyses Computer System, NASA SP-260, 1971.